Water availability drives signatures of local adaptation in whitebark pine (*Pinus albicaulis* Engelm.) across fine spatial scales of the Lake Tahoe Basin, USA

BRANDON M. LIND,* CHRISTOPHER J. FRIEDLINE,† JILL L. WEGRZYN,‡
PATRICIA E. MALONEY,§ DETLEV R. VOGLER,¶ DAVID B. NEALE** and ANDREW J. ECKERT†
*Integrative Life Sciences Program, Virginia Commonwealth University, Richmond, VA 23284, USA, †Department of Biology, Virginia Commonwealth University, Richmond, VA 23284, USA, ‡Department of Ecology and Evolutionary Biology, University of Connecticut, Storrs, CT 06269, USA, §Department of Plant Pathology and Tahoe Environmental Research Center, University of California, Davis, CA 95616, USA, ¶USDA, Forest Service, Pacific Southwest Research Station, Institute of Forest Genetics, 2480 Carson Road, Placerville, CA 95667, USA, **Department of Plant Sciences, University of California, Davis, CA 95616, USA*

Abstract

Patterns of local adaptation at fine spatial scales are central to understanding how evolution proceeds, and are essential to the effective management of economically and ecologically important forest tree species. Here, we employ single and multilocus analyses of genetic data (n = 116 231 SNPs) to describe signatures of fine-scale adaptation within eight whitebark pine (*Pinus albicaulis* Engelm.) populations across the local extent of the environmentally heterogeneous Lake Tahoe Basin, USA. We show that despite highly shared genetic variation (F_{ST} = 0.0069), there is strong evidence for adaptation to the rain shadow experienced across the eastern Sierra Nevada. Specifically, we build upon evidence from a common garden study and find that allele frequencies of loci associated with four phenotypes (mean = 236 SNPs), 18 environmental variables (mean = 99 SNPs), and those detected through genetic differentiation (n = 110 SNPs) exhibit significantly higher signals of selection (covariance of allele frequencies) than could be expected to arise, given the data. We also provide evidence that this covariance tracks environmental measures related to soil water availability through subtle allele frequency shifts across populations. Our results replicate empirical support for theoretical expectations of local adaptation for populations exhibiting strong gene flow and high selective pressures and suggest that ongoing adaptation of many *P. albicaulis* populations within the Lake Tahoe Basin will not be constrained by the lack of genetic variation. Even so, some populations exhibit low levels of heritability for the traits presumed to be related to fitness. These instances could be used to prioritize management to maintain adaptive potential. Overall, we suggest that established practices regarding whitebark pine conservation be maintained, with the additional context of fine-scale adaptation.

Keywords: linkage disequilibrium, local adaptation, *Pinus albicaulis*, Sierra Nevada, water availability

Received 13 September 2016; revision received 3 March 2017; accepted 6 March 2017

Correspondence: Brandon M. Lind, Fax: 804-828-0820;
E-mail: lindb@vcu.edu
Data reference numbers (PRJNA377566).

Introduction

The study of local adaptation has been an integral part of evolutionary biology as a whole, as local adaptation influences a wide variety of biological patterns and

processes (reviewed in Savolainen *et al.* 2013). Trees in particular have received much attention in this regard because many species are ecologically and economically important, and high outcrossing rates (Neale & Savolainen 2004) result in large effective population sizes (which increase the effectiveness of selection) as well as weak neutral genetic differentiation (which decreases the confounding effects of selection and population structure). Together, these circumstances create ideal conditions in which to detect selective processes in nature (Savolainen & Pyhäjärvi 2007). Investigators seeking to explain the genetic basis of local adaptation in trees, and plants in general, have been motivated by observations of significant differentiation for quantitative genetic variation across populations (e.g., Q_{ST}) where the underlying loci may be differentiated among populations as well (Endler 1977; reviewed in Storz 2005; Haasl & Payseur 2016). In these cases, loci contributing to local adaptation could be identified through genetic indices of differentiation, or by targeting trait or environmentally associated loci that stand out above background demography. Yet, theoretical (Latta 2003; Le Corre & Kremer 2003) and empirical (Hall *et al.* 2007; Luquez *et al.* 2007) investigations have shown that discordance between Q_{ST} and F_{ST} of causative loci can occur under adaptive evolution. Moreover, as the number of underlying loci increases, the divergence between these indices increases as well, and the contribution of F_{ST} to any individual underlying locus decreases. In cases that exhibit strong diversifying selection and high gene flow, this adaptive divergence results from selection on segregating genetic variation (Hermisson & Pennings 2005; Barrett & Schluter 2008; reviewed in Tigano & Friesen 2016) and is attributable to the among-population component of linkage disequilibrium (Ohta 1982; Latta 1998). In the short term, local adaptation will be realized through subtle coordinated shifts of allele frequencies across populations causing covariance (i.e., LD) among many underlying loci (Latta 1998, 2003; Barton 1999; McKay & Latta 2002; Kremer & Le Corre 2012; Le Corre & Kremer 2012), such that adaptation need not take place through numerous fixation events or sweeping allele frequency changes (Mackay *et al.* 2009; Pritchard & Di Rienzo 2010). Over many thousands of generations, these shifts can lead to concentrated architectures of large-effect loci with a reduction of those with small effect (Yeaman & Whitlock 2011). For studies investigating continuous phenotypes such as those often related to fitness, even among populations with highly differentiated phenotypic traits sampled under a robust design (Lotterhos & Whitlock 2015), it may be difficult to identify many of the loci underlying the quantitative trait in question. Thus, for many species,

specifically across fine spatial scales, the signal of local adaptation within much of current genetic data may go largely undetected using only single-locus approaches (Latta 1998, 2003; Le Corre & Kremer 2003; Yeaman & Whitlock 2011; Kemper *et al.* 2014), resulting in calls for theory and empiricism that move beyond single-locus perspectives (Pritchard & Di Rienzo 2010; Sork *et al.* 2013; Tiffin & Ross-Ibarra 2014; Stephan 2015).

Populations of forest trees, particularly conifers, have a rich history of common garden, provenance tests and genecological studies that demonstrate abundant evidence for local adaptation among populations, even over short geographic distances (e.g., Mitton *et al.* 1989, 1998; Budde *et al.* 2014; Csilléry *et al.* 2014; Vizcaíno-Palomar *et al.* 2014; Eckert *et al.* 2015; Holliday *et al.* 2016; Roschanksi *et al.* 2016) providing further support that fine spatial scales are relevant to adaptation (Richardson *et al.* 2014). This extensive history has also revealed the highly polygenic nature of adaptive traits (Langlet 1971; Holland 2007). Even so, the majority of these investigations have been limited to single-locus perspectives using either candidate genes (e.g., González-Martínez *et al.* 2008; Eckert *et al.* 2009) or a large set of molecular markers (e.g., Eckert *et al.* 2010) to explain the genetic basis of local adaptation. In most cases, a few loci underlying the adaptive trait in question are identified and generally explain a small-to-moderate proportion of the overall heritability of the trait (Neale & Savolainen 2004; Savolainen *et al.* 2007; Ćalić *et al.* 2016). Yet because of the presumed polygenic nature underlying these adaptive phenotypic traits, and because past investigations have generally applied single-locus perspectives, informative biological signals may therefore be overlooked, and it is likely that a majority of the genetic architecture of local adaptation in trees remains undescribed (Savolainen *et al.* 2007; Sork *et al.* 2013; Ćalić *et al.* 2016).

Spurred in part by the advance of theory and availability of genomewide marker data, attention has been refocused to describe underlying genetic architectures from a polygenic perspective. This transition began in model organisms (e.g., Turchin *et al.* 2012) and has expanded to other taxa such as stick insects (Comeault *et al.* 2014, 2015), salmon (Bourret *et al.* 2014) and trees (Ma *et al.* 2010; Csilléry *et al.* 2014; Hornoy *et al.* 2015). Indeed, species that occupy landscapes with high degrees of environmental heterogeneity offer exemplary cases with which to investigate local adaptation. Near its southern range limit, whitebark pine (*Pinus albicaulis* Engelm.) populations of the Lake Tahoe Basin (LTB) inhabit a diversity of environmental conditions. As exemplified by the strong west-to-east precipitation gradient (see Fig. 1), many of the environmental
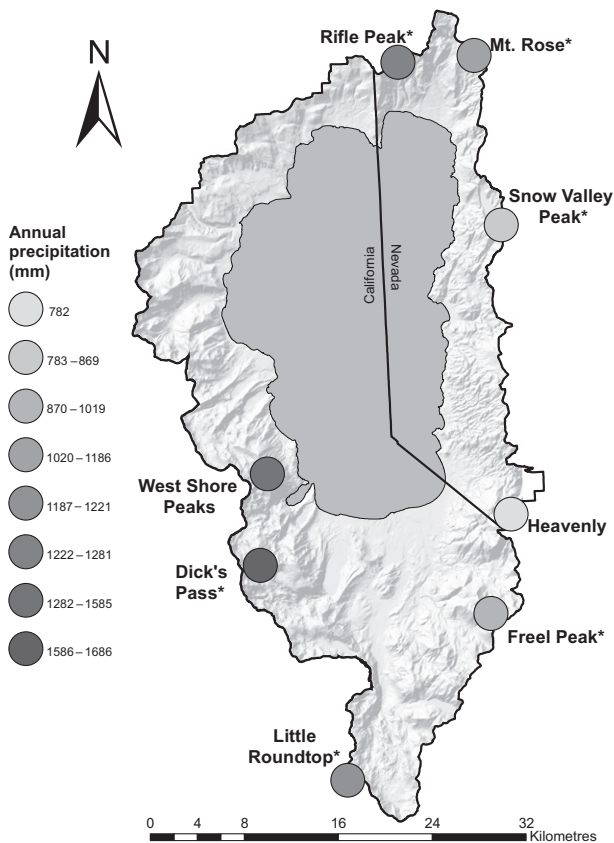
Fig. 1 Populations used for sampling *P. albicaulis* within the Lake Tahoe Basin (dark outline). Annual precipitation is given for each population to demonstrate the west–east rain shadow experienced across fine spatial scales. Asterisks indicate populations in the common garden study.

characteristics of the LTB vary over short physical distances (<1 km) and have the potential to shape geographic distributions of *P. albicaulis* at spatial scales below those typically investigated (i.e., range-wide studies) for forest trees. Local spatial scales are of particular interest to resource and conservation agencies as this is the scale at which most management is applied. Here, we build upon past work from a common garden (P.E. Maloney, D.R. Vogler, A.J. Eckert, C.E. Jensen, A. Delfino-Mix, in review) to investigate the genetic architecture of fine-scale local adaptation across *P. albicaulis* populations of the LTB by exploring the relationships between genotype, 18 environmental variables and five fitness-related phenotypic traits using both single and multilocus approaches. Specifically, we use the *P. albicaulis* populations of the LTB to address the following three questions: (i) Is there evidence that a long-lived, outcrossing plant species exhibiting high levels of gene flow can be locally adapted across fine spatial scales?

(ii) What is the genetic basis and relationship among loci underlying adaptation in such a species? (iii) How similar are the genetic bases of fitness-related phenotypes to the loci putatively under selection from the environment? Using this information, we will contextualize how instances of fine-scale adaptation have management implications. This study highlights the advantages of a polygenic perspective and investigates signatures of local adaptation using a large set of null markers to determine the extremity of allele covariance among putatively adaptive loci where others have relied on simulation or null candidate genes. Furthermore, this work provides additional empirical evidence for theoretical predictions of covariance among adaptive loci found by other studies in trees.

Materials and methods

Focal species, study area, and sampling

A foundation species of subalpine, high elevation forests in California and Nevada, *Pinus albicaulis* plays a vital role in ecosystem function and services including food resources for wildlife, forest cover, watershed protection, protracting snowmelt and biodiversity [see references in Mahalovich & Stritch (2013), Tomback *et al.* (2016)]. It is threatened by fire-suppression, climate change, the non-native pathogen white pine-blister rust, caused by *Cronartium ribicola* J. C. Fisch., and mountain pine beetle, *Dendroctonous ponderosae* Hopkins (Tomback & Achuff 2010; Mahalovich & Stritch 2013).

The LTB lies within California and Nevada and experiences a Mediterranean climate. Precipitation falls during the winter months, most often in the form of snow, with a strong west–east gradient (Fig. 1). Each of the eight study populations (three subplots per population) was located in a distinct watershed and distributed around the Basin to capture variation in the physical environment (e.g., climate, geology, and topography). Needle tissue was sampled in 2008 from 244 *P. albicaulis* trees (Table 1). From these eight populations, six populations were chosen to sample cones from 88 of the 244 trees that were sampled for needle tissue. All samples were collected from trees separated by 30–1000 m, with an average interpopulation distance of 31 km. Universal Transverse Mercator coordinates, elevation, slope, and aspect (USDA Forest Service FHTET) were used with the PRISM climatic model (Daly *et al.* 1994) to determine climatic parameters of sampled areas from 1971 to 2000, while soil survey data (United States Department of Agriculture, Natural Resources Conservation Service 2007) were used to describe the edaphic conditions of the LTB (Table 1).

Common gardens and phenotypic measurements

Fitness-related traits related to survival, especially during seedling and juvenile stages, are an important component of total lifetime fitness (e.g., Postma & Ågren 2016), particularly for forest trees, and are likely to be composed of phenotypic traits related to growth, phenology, resource allocation patterns, water-use efficiency, and disease susceptibility. To estimate early-lifetime phenotypes of mother trees, seeds sampled from 11 to 19 maternal trees ($n = 88$) located in six of the eight populations were established in a common garden (Table 1) using a random block design (for further details, see P.E. Maloney, D.R. Vogler, A.J. Eckert, C.E. Jensen, A. Delfino-Mix, in review). Growth (height), phenology (bud flush), water-use efficiency ($\delta^{13}C$), and resource allocation [root: shoot biomass, $N(\mu g)$] were measured when seedlings reached ~2 years in age (see P.E. Maloney, D.R. Vogler, A.J. Eckert, C.E. Jensen, A. Delfino-Mix, in review for details). Height was recorded in April and October 2011, while two seedlings per family per block were harvested, clipped above the root collar, dried, and weighed to determine root and shoot biomass. For $\delta^{13}C$ and $N(\mu g)$ analysis, needle tissue from one seedling per family per block was harvested, coarsely ground, and dried at 60 °C for 96 h. Between 2 and 3 mg of tissue per sample was sent to the Stable Isotope Facility at UC Davis for isotope analyses (http://stableisotopefacility.ucdavis.edu/).

DNA extraction, sequencing and analysis

Total genomic DNA was isolated from needle tissue sampled from 244 trees across all eight populations using the Qiagen DNEasy 96 Plant kit according to protocol (Qiagen, Germantown, MD). Restriction site-associated double digests of total genomic DNA using MseI and EcoRI enzymes (ddRADSeq, Peterson *et al.* 2012) were used to prepare three multiplexed, barcoded libraries of up to 96 individuals each, as in Parchman *et al.* (2012). Using the QIAquick Gel Extraction Kit (Qiagen), amplified fragments were then isolated near 400 bp of pooled PCR product separated in an agarose gel. Single-end sequencing of libraries was carried out on the Illumina HiSeq 2500 platform with a single library per flowcell lane. For added coverage, each library was sequenced twice using 50-bp reads and twice for 150-bp reads, except Library 3 which was sequenced 4× for 150-bp reads to increase optimality of the mapping reference individual. All sequencing was performed at the DNA Sequencing Facility of the University of California at Berkeley (https://mcb.berkeley.edu/barker/dnaseq/home). After calling genotypes, SNPs, and further filtering (see Supporting Information), we judged the veracity of our sequence data by mapping the empirical set of SNPs against the sugar pine (*P. lambertiana* Dougl.) reference genome (version 1.0) using 85% similarity and 50% length coverage thresholds

Table 1 Population location and associated attributes. Population size – total (maternal trees with seedlings in common garden). Climatic values were ascertained from data spanning 1971–2000. Ann. precipitation, annual precipitation; AWC, available water capacity at 25 or 50 cm soil depth; CEC, cation exchange capacity; GDD, growing degree days above 5 °C; Max solar rad input, maximum solar radiation input; WC-15 bar, water capacity at −15 bar (wilting point); WC-⅓bar – water capacity at −⅓bar (field capacity)

	Dick's pass*	Freel peak*	Heavenly	Little round top*	Mt. rose ophir*	Rifle peak*	Snow valley peak*	West shore peaks
Population size	25 (15)	48 (19)	25 (0)	25 (14)	49 (11)	24 (15)	24 (14)	24 (0)
Ann. precipitation (mm)	1686	1019	782	1221	1186	1281	869	1585
AWC-25 cm (kPa)	1.66	1.57	1.12	1.97	1.95	1.89	2.66	1.20
AWC-50 cm (kPa)	2.75	2.38	2.00	2.93	2.75	3.11	4.22	2.02
CEC (cmol$_c$·kg^{-1})	0.00	1.45	0.00	12.50	2.90	0.00	0.00	0.00
Clay (%)	6.50	4.50	6.70	14.60	3.00	6.75	6.80	6.00
Elevation (m)	2806	2865	2851	2875	2717	2819	2740	2780
GDD-Aug (days)	295	190	276	211	296	235	289	279.5
GDD-May (days)	0	0	6	0	11	0	2	1
Max solar rad input (%)	83.59	79.03	78.40	80.09	90.61	93.28	71.70	76.43
Max Temp – July (°C)	21.1	21.6	23.2	21.5	22.9	22.7	23.4	21.8
Min. Temp – Jan (°C)	−6.5	−8.8	−7.5	−8.0	−7.4	−7.4	−7.7	−6.6
Rock coverage (%)	31.00	18.67	25.00	14.67	7.00	30.00	26.67	42.67
Sand (%)	77.67	87.80	83.50	66.20	90.60	74.00	64.50	85.00
Silt (%)	15.8	7.7	9.7	19.1	6.4	19.2	28.7	9.0
WC-15 bar (kPa)	6.6	4.0	3.3	3.6	5.5	8.7	14.0	2.5
WC-⅓ bar (kPa)	9.7	8.0	8.4	7.3	9.8	11.4	14.4	6.2

*Populations from which seeds sampled from cones were planted in a common garden. Environmental variables are averaged across subplots.

(http://dendrome.ucdavis.edu/ftp/Genome_ Data/ge nome/pinerefseq/Pila/v1.0/).

Identifying focal sets of loci

To identify genotype–environmental associations, we implemented BAYENV2 (version 2.0; Coop *et al.* 2010; Günther & Coop 2013), a Bayesian single-locus approach that accounts for population history before performing association analysis (Coop *et al.* 2010). To ensure convergence, we ran five independent chains of BAYENV2 using the empirical SNPs ($n = 116\,231$), with 100 000 iterations for each SNP within each chain. MCMC convergence across chains was inspected using the CODA library in R (R Core Team 2015). For each SNP, we calculated the harmonic mean across chains for the Bayes factor ($\overline{BF}$) and absolute value of Spearman's ρ (hereafter $\overline{\rho_S}$). When calculating $\overline{BF}$, if a particular SNP returned Bayes factors greater than one for at least 3/5 chains, we would take the harmonic mean from this subset to avoid underestimation of the Bayes factor. However, if this was not the case ($\overline{BF} > 1$ in ≤2/5 chains), we would take the harmonic mean from the values that were less than or equal to one. We identified focal SNPs by the intersection between the upper tail (99.5th percentile) of $\overline{BF}$ and the upper tail (99th percentile) of the absolute value of $\overline{\rho_S}$, as recommended in the BAYENV2 manual (version 2.0; page 4).

To associate genotype with phenotype, we implemented a Bayesian sparse linear mixed model (BSLMM) from the GEMMA software package (Zhou *et al.* 2013). BSLMM is a hybrid of LMM and Bayesian variable selection regression (BVSR) that also offers considerable statistical advantages over single-locus GWAS approaches (Guan & Stephens 2011; Ehret *et al.* 2012; Zhou *et al.* 2013; Moser *et al.* 2015). Specifically, to describe the underlying genetic architecture, BSLMM uses priors (described below) and attributes of the genetic data to estimate the number of underlying SNPs (N_{SNP}), the posterior inclusion probability (γ, hereafter *PIP*) for individual SNPs as well as the proportion of phenotypic variance explained by the polygenic and sparse effects of each SNP (*PVE*).

Before input to GEMMA, the empirical set of SNPs was reduced to include only those individuals with seedlings in the common garden ($n = 88$) and loci which had MAF below 0.01 due to this reduction were eliminated alongside monomorphic SNPs. For each phenotype, we ran four independent chains for the BSLMM, with 1000 000 warm-up steps and 50 000 000 steps in the MCMC, sampled every 1000th step. Priors for *PVE* by the model, h, were set as [0.01,0.9], and the $\log_{10}$ inverse number of SNPs, $\log_{10}(1/p)$, [−3.0,0.0], which equates to between 1 and 300 underlying loci (N_{SNP}).

Convergence of the MCMC across chains was inspected using the CODA library in R. To summarize the GEMMA output, we report means and 95% credible intervals for *PVE* and N_{SNP} from the posterior distributions. To assess significance of association of a SNP to a phenotype, we used the *PIP* from all four independent chains to calculate the harmonic mean ($\overline{PIP}$) and chose SNPs that were greater than or equal to the 99.9th percentile of $\overline{PIP}$ ($n \approx 116$ SNPs/phenotype) for each phenotype. We also explored SNPs with $\overline{PIP} \geq$ 99.8th percentile ($n \approx 232$ SNPs/phenotype).

We implemented the program OUTFLANK (Whitlock & Lotterhos 2015) to investigate loci identified as outliers based on population genetic structure (e.g., F_{ST}). Using this approach, and excluding loci with expected heterozygosity values below 10% with subsequent trimming of the lower and upper 5% of empirical F_{ST} values, we inferred a null distribution of F'_{ST} and identified outlier loci with a false discovery rate of 5% from the empirical set of SNPs.

Inferring signatures of local adaptation

To determine whether individual sets of focal loci (identified from GEMMA, BAYENV2, and OUTFLANK analyses) collectively exhibited elevated signatures of selection acting across multiple loci, we investigated the level of allele frequency covariance among all SNP pairs within each focal set. For instance, to calculate the covariance of allele frequencies across populations between two SNPs, SNP$_i$ and SNP$_j$, within a focal set of SNPs associated with a particular phenotype in GEMMA, we used the global minor allele of each SNP, q, according to the interpopulation component of linkage disequilibrium,

$$\hat{D}_{a(ij)} = \sum_k \frac{n_k}{n}(q_{i,k}q_{j,k} - q_i q_j) \qquad (1)$$

where n_k is the number of individuals in population k, n is the global population size, $q_{i,k}$ is the allele frequency of the ith SNP in population k, $q_{j,k}$ is the allele frequency of the jth SNP in population k, while q_i and q_j are the respective global allele frequencies of the ith and jth SNP across $k = 6$ populations (Storz & Kelly 2008, their Equation 2; Ma *et al.* 2010, their Equation 3). Because we chose the allele to use in comparisons based on global minor allele frequency, all calculations of $\hat{D}_{a(ij)}$ are therefore referenced to the global minor allele haplotype for a pair of SNPs. For populations that experience high levels of gene flow and divergent phenotypic optima due to selection, $\hat{D}_{a(ij)}$ is expected to be positive between allele frequencies of loci conferring a positive effect on the phenotype, negative between

those conferring opposite effect and zero between (conditionally) neutrally loci (eq. [6] in Latta 1998). Because we were not able to discern the direction of effect for alleles within each population (as in, e.g., Gompert *et al.* 2015) and to facilitate comparison among analyses, we identified selective signatures by calculating the absolute value of $\hat{D}_{a(ij)}$ for each locus pair. We also calculated $\hat{D}_{a(ij)}$ for focal SNPs associated with environmental variables from BAYENV2 and those identified as outliers from OUTFLANK. In these two cases, we used allele frequencies across all eight populations.

To be able to discern if the level of covariance of allele frequencies among SNPs within a set identified by GEMMA (or another method, hereafter focal SNPs) was greater than that from SNPs randomly chosen from our data set (i.e., than expected given the data), we first separated all SNPs in the data set by their expected heterozygosity into bins of 0.01 ranging from 0 to 0.50 (e.g., a SNP with H_E of (0.000–0.010] would be binned into the first bin, while an H_E of (0.490–0.500] would be binned into the 50th). We then created a set of SNPs from which to take randomized draws by subtracting the focal SNPs from the full set of SNPs. Next, based on the occupancy of heterozygosity bins for a given focal set, we randomly selected remaining SNPs to create a null set. We chose SNPs randomly in this way, 1000 times, each time calculating the absolute value of $\hat{D}_{a(ij)}$ among SNP pairs within each set. From each of these 1000 distributions, we calculated 1000 median absolute $\hat{D}_{a(ij)}$ values to create a null distribution for use in comparison with the median absolute $\hat{D}_{a(ij)}$ from the focal set of SNPs. If the median $\hat{D}_{a(ij)}$ is greater among our focal SNPs than the 95th percentile of the null distribution of 1000 medians, we will conclude that the signature of selection among loci within our focal sets is greater than could have arisen by chance, given the data.

To infer signatures of allele frequency shifts associated to environment, we implemented an approach similar to eqn 1, but instead of estimating $\hat{D}_{a(ij)}$ across all populations we estimated $\hat{D}_{a(ij)}$ across populations in a pairwise fashion (hereafter $pw\hat{D}_{a(ij)}$) using focal SNPs from a given method. In this case, we calculated global allele frequency (q_i or q_j) based on the frequency of allele q across the $k = 2$ populations (pop_l and pop_m) under consideration (where $n_l + n_m = n$). From these estimates, we created a symmetric matrix of $pw\hat{D}_{a(ij)}$ with columns and rows for populations, and distances within the diagonal set to zero. We then implemented Mantel tests (Mantel 1967) using $pw\hat{D}_{a(ij)}$ matrices against other population pairwise distance matrices such as geographic distance inferred using great circle distances (km) following Vincenty's method, and Euclidian distance matrices for each of the five phenotypes and 18 environmental variables. Because we chose to take absolute values of $pw\hat{D}_{a(ij)}$ for each locus pair

(as with $\hat{D}_{a(ij)}$), we note that the sign of the correlation coefficient, r, from Mantel tests may reflect the opposite directionality for any given SNP pair. Mantel tests were run with 9999 iterations using the SKBIO package (version 0.4.2) in PYTHON. Each environmental or phenotypic value was centred and standardized across populations before calculating Euclidian distances, but not for $pw\hat{D}_{a(ij)}$ or geographic distance matrices. For each set of focal SNPs associated with phenotype or environment, we also quantified the mean allele frequency differences across populations and compared this to 1000 sets of random SNPs chosen by H_E.

Results

SNP filtering and characterization

After calling genotypes, SNPs and filtering (see results section of Supporting Information), we retained 116 231 imputed SNPs for use as the empirical set in downstream analyses (Table S1, Supporting information). Of these contigs, 107 354 (92.4%) mapped to the *P. lambertiana* reference genome, thus lending authenticity to our sequence data. However, we avoid further discrimination of loci for (proximity to) genic regions until a future genome update with increased curation and density of annotation.

Overall, populations show little genetic structure with plots accounting for less than 1% of the variance in allele frequencies ($F_{\text{plot,total}} = 0.00687$; 95% credible interval: 0.0067–0.0070). Of this variation, 56.6% was accounted for by populations ($F_{\text{pop,total}} = 0.00389$; 95% CI: 0.0038–0.0040) with the remainder due to plots within populations ($F_{\text{plot,pop}} = 0.00299$; 95% CI: 0.0029–0.0031). We found similar patterns among the locus-specific estimates of F_{ST} (Fig. S1, Supporting information). Moreover, we found no discernible clustering of populations using PCA (following Patterson *et al.* 2006), respectively, accounting for 5.6% and 1.2% of the variance in allele frequencies (Fig. S2, Supporting information). To further address applicability of the island model used for calculation of $\hat{D}_{a(ij)}$ and $pw\hat{D}_{a(ij)}$, we analysed population pairwise F_{ST} according to Weir & Cockerham (1984) using the HIERFSTAT package in R. Results show little differentiation among populations (mean = 0.005, max = 0.016) with no evidence of isolation by distance (Mantel's $r = 0.0990$, $P = 0.2310$).

Genotype–environment analyses

To explore the degree of association among environmental variables between populations, we used Mantel tests between Euclidian environmental distance matrices. In most cases, we found significant correlations

with many of the edaphic variables measured for this study, as well as between latitude and elevation (r = 0.3988, P = 0.0490), longitude and annual precipitation (r = 0.7145, P = 0.0030), and between per cent maximum solar radiation and latitude distances (r = 0.4629, P = 0.0370; Table S2, Supporting information). Additionally, geographic distance among populations was only associated with latitude (r = 0.9631, P = 0.001), per cent maximum solar radiation input (r = 0.3992, P = 0.0468), and elevation (r = 0.4062, P = 0.0452), the three of which were correlated environmentally (Table S2, Supporting information), but not to any of the remaining environmental variables (Mantel tests P > 0.3131, data not shown).

Through the intersection of the top 0.5% of $\overline{BF}$ and top 1% of $\overline{\rho_S}$, BAYENV2 analysis revealed between 14 (CEC) and 157 (GDD-Aug) focal SNPs associated with environment (Table S3, Supporting information). However, when calculating the $\overline{BF}$ for each SNP, it was never the case that more than two of the five chains produced BF >1, of which chains with large values were driven primarily by seed number (we used additional seed numbers for a small subset of the data during exploration, data not shown). The range of $\overline{\rho_S}$ across all focal SNPs across all environments varied from a minimum of 0.138 to a maximum 0.345 (Table S3, Supporting information). Additionally, the focal SNPs identified by BAYENV2 displayed a bias towards SNPs with low values of H_E (Figs S3–S4, Supporting information, see results section of Supporting Information) when compared to the distribution from the full set of SNPs (Fig. S5, Supporting information). As such, our environmental associations should be interpreted with caution, as we did not have any SNPs with $\overline{BF}$ >1 nor do our harmonic mean nonparametric correlations exceed 0.35. Even so, when we compared absolute estimates of $\hat{D}_{a(ij)}$ among focal SNPs against the corresponding 1000 null sets of loci, we found that for all focal sets, the median $\hat{D}_{a(ij)}$ was always greater than the 100th percentile of the null distribution (Table S3, Supporting information; Fig. 2). The magnitude of this difference varied across environmental variables, being the smallest for per cent clay (1.17×) and largest for annual precipitation (5.10×, Table S3, Supporting information). Upon comparison of focal and null sets in both the distribution of single-locus and multilocus F_{ST}, focal sets were representative of single-locus estimates of the null sets (Figs S6–S7, Supporting information) and generally greater than the distribution of multilocus F_{ST} than the null (Figs S8–S9, Supporting information). Single-locus results suggest that many focal SNPs are unlikely outliers for F_{ST}, while multilocus comparisons exemplify the elevated frequency covariance of SNPs in focal sets. These data demonstrate that for most environmental variables, the

focal SNPs show higher degrees of $\hat{D}_{a(ij)}$ than could be expected, given the data, despite having low $\overline{BF}$ and $\overline{\rho_S}$.

Through the examination of patterns of allele frequency shifts ($pw\hat{D}_{a(ij)}$) across loci associated with environment, we found no significant associations with geographic distance using Mantel tests (P > 0.1116). While this suggests the absence of linear allelic clines, it does not necessarily preclude the presence of environmental gradients or correlated patches as suggested by environmental distance associations (Table S2, Supporting information). When we investigated the association between $pw\hat{D}_{a(ij)}$ matrices against the eponymous environmental distance matrix, we found significant association for annual precipitation, GDD-May, longitude, per cent rock coverage, per cent sand, minimum January temperature and field capacity (WC-⅓bar; all r > 0.4806; P = 0.0361; Table 2). Additionally, we examined relationships between a particular $pw\hat{D}_{a(ij)}$ matrix and the 17 remaining environmental distance matrices and found significant associations in an additional 13 comparisons (Table 2), with five of these comparisons having $pw\hat{D}_{a(ij)}$ associated with either annual precipitation or longitudinal Euclidian distance. We also observed shifts of alleles associated with longitude or soil water capacity across six of the remaining eight significant associations (Table 2), with the remaining two significant associations among edaphic conditions of sand, silt, or clay. The magnitude of the mean allele frequency difference across populations of focal SNPs was subtle as expected (range 0.018–0.029) and was generally slightly larger than that predicted from random SNPs of the same heterozygosity (Figs S10–S11, Supporting information). Overall, our results indicate that the vast majority of subtle allele frequency shifts among loci associated with environment ($pw\hat{D}_{a(ij)}$) have significant associations related to interpopulation distances of water availability (Table 2).

Genotype–phenotype analyses

Phenotypic traits were heritable and structured across populations (bud flush h^2 = 0.3089, Q_{ST} = 0.0156; δ^{13}C h^2 = 0.7787, Q_{ST} = 0.0427; height h^2 = 0.0608, Q_{ST} = 0.0418; N(µg) h^2 = 0.3525, Q_{ST} = 0.0191; root:shoot h^2 = 0.3240, Q_{ST} = 0.0110; Table S4, Supporting information) and were correlated with environmental variables (both climate and soil) in ways unexplainable by neutral evolutionary forces (P.E. Maloney, D.R. Vogler, A.J. Eckert, C.E. Jensen, A. Delfino-Mix, in review). Additionally, bud flush and δ^{13}C had significant Q_{ST} > F_{ST} (P.E. Maloney, D.R. Vogler, A.J. Eckert, C.E. Jensen, A. Delfino-Mix, in review, using the genetic data presented herein). We used a subset of the empirical set of SNPs for use in genotype–phenotype analysis, after filtering
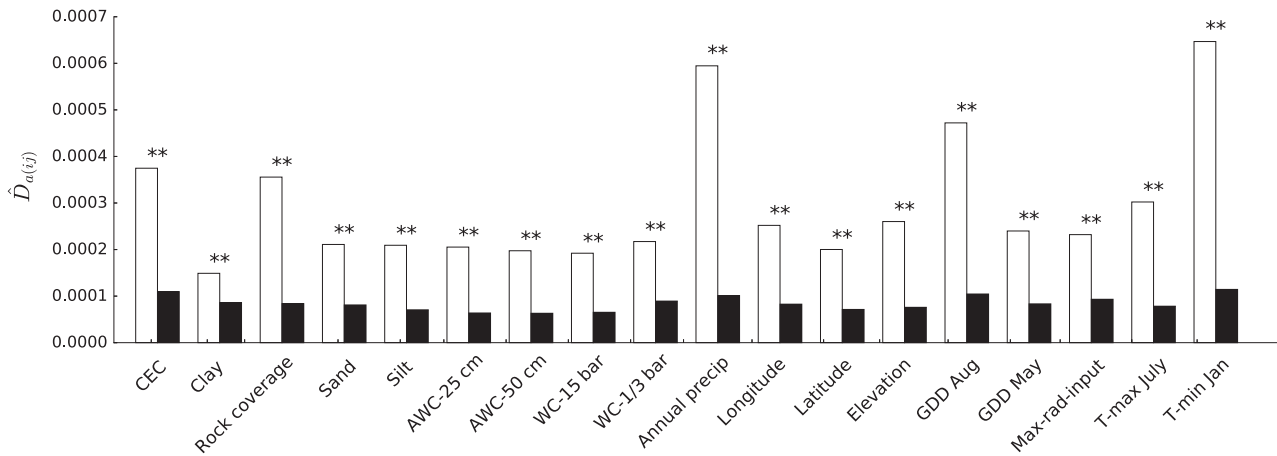
Fig. 2 Allele frequency covariance ($\hat{D}_{a(ij)}$) among loci associated to environment by BAYENV2. In white are the median values from $\hat{D}_{a(ij)}$ calculated among focal SNPs associated with environment. Black bars display the 95th percentile of the null distribution of median $\hat{D}_{a(ij)}$. Environmental variables are grouped by those related to soil (CEC through WC-1/3 bar) and those related to either climate or geography (Annual precipitation through T-min Jan), with variables related to water availability grouped together in the centre of the figure (AWC-25 cm through Annual precipitation). All sets of focal loci had median $\hat{D}_{a(ij)}$ greater than the 100th percentile of the null distribution, as indicated by two stars (**). Environmental variables as in Table 1.

we retained 115 632 SNPs. PCA revealed a similar pattern to the empirical set of SNPs (data not shown). Using three significant axes of population structure identified through Tracy–Widom tests, we associated SNPs to phenotypes with BSLMM (Zhou *et al.* 2013) using the top 99.9th and 99.8th percentiles of $\overline{PIP}$ (Fig. 4, Table S5, Fig. S12, Supporting information). From observations of density and trace plots, we concluded that the posterior distributions across chains were converging (not shown). The H_E of focal loci was generally representative of the empirical set (Figs S13–S14, Supporting information).

Overall, the genetic variance of SNPs included in the polygenic model explained between 14.4% [N (μg)] and 37.6% (root:shoot) of the variance in the phenotypes measured in our study (PVE, Fig. 3, Table S4, Supporting information). For many of the measured phenotypes, a considerable proportion of the narrow sense heritability estimated previously was therefore accounted for in the estimates of PVE (Table S4, Supporting information), as should be the case with sufficient genetic sampling (Gompert *et al.* 2016). Interestingly, in the case of height, PVE exceeded the upper confidence interval of the estimated h^2 (Table S4, Supporting information).

To acquire estimates of PVE from genotype–phenotype associations using single-locus approaches, we used univariate linear mixed models implemented in GEMMA (see Supporting Information, Table S6, Supporting information). Across all phenotypes, there were no loci that exceeded the adjusted threshold for inclusion calculated from q-values with an FDR of 0.05 (Storey *et al.* 2015; version 2.4.2), with the minimum q-

value across SNPs within phenotypes ranging between 0.2046 (δ^{13}C) and 0.9999 [N(μg)] (Table S6, Supporting information). Except for root:shoot biomass, the maximum-likelihood estimates of PVE differed drastically from the estimates from BSLMM, with PVE never exceeding 1.08e−06 suggesting that a larger proportion of the heritable genetic variation for the traits measured here is explained by multiple SNPs than by individual SNPs alone. Finally, to determine whether LMM loci near the threshold were captured by the BSLMM for a particular phenotype, we isolated the loci from univariate LMM above a reduced threshold of $-\ln(p_{\text{Wald}}) \geq 10$ (see Fig. S15, Supporting Information). By this reduced threshold, we identified one unique locus for both bud flush and N(μg), four unique loci for both height and root:shoot biomass and five unique loci for δ^{13}C (15 unique loci overall). We examined the focal loci sets identified from the 99.9th percentile of $\overline{PIP}$ in BSLMM for these LMM reduced-threshold loci and found 1 of the 4 LMM loci for both root:shoot biomass and height and 2 of the 5 loci for δ^{13}C. When we assessed the set of loci in the 99.8th percentile of BSLMM, we recovered all LMM reduced-threshold loci for bud flush and N(μg) ($n = 1$), 1 of 4 loci for root:shoot biomass, 3 of 4 loci for height, and 3 of 5 loci for δ^{13}C.

To determine whether focal loci associated with phenotype by BSLMM exhibited evidence of selection, we estimated allele frequency covariance ($\hat{D}_{a(ij)}$) among focal SNPs and compared these estimates to 1000 null sets of SNPs. We found evidence for elevated covariance among the 99.9th percentile of $\overline{PIP}$ loci associated with bud flush and root:shoot biomass (Fig. 4A,

Table 2 Signatures of allele frequency shifts associated with environmental distance. Significant Mantel tests (9999 permutations) from comparisons among $pw\hat{D}_{a(ij)}$ matrices from SNPs associated with environment (first column) against environmental Euclidian distance (second column). Environmental variables as in Table 1

$pw\hat{D}_{a(ij)}$	Environmental Euclidian distance	Mantel's r	P-value
Ann. precipitation*	Ann. precipitation	0.7135	0.0027
Longitude*	Longitude	0.6522	0.0024
Longitude*	Ann. precipitation	0.7716	0.0016
Rock coverage*	Ann. precipitation	0.5542	0.0221
Tmin-Jan*	Ann. precipitation	0.5765	0.0132
Longitude*	Latitude	−0.4257	0.0347
Rock coverage*	Longitude	0.5566	0.0284
Tmin-Jan*	Longitude	0.4822	0.0273
WC-15 bar*	Tmax-July	0.3490	0.0309
WC-⅓bar*	WC-⅓bar	0.4806	0.0361
WC-⅓bar*	Tmax-July	0.4539	0.0037
WC-⅓bar*	AWS0-25	0.4329	0.0384
WC-⅓bar*	AWS0-50	0.4538	0.0464
WC-⅓bar*	WC-15 bar	0.5126	0.0335
GDD-May	GDD-May	0.8480	0.0013
Rock coverage	Rock coverage	0.5124	0.0145
Sand	Sand	0.5574	0.0046
Tmin-Jan	Tmin-Jan	0.5791	0.0137
Sand	Clay	0.5345	0.0232
Silt	Sand	0.4408	0.0238

*A comparison in which at least one variable is water-related, or was associated with annual precipitation.

Fig. 3 Violin plots for the kernel density estimator of the posterior distributions (light grey) taken from Bayesian sparse linear mixed models (BSLMM) executed in GEMMA for (A) the proportion of variance explained by SNPs included in the model (PVE) and (B) the number of SNPs underlying the phenotypic trait (N_{SNP}). Priors for N_{SNP} and PVE were [1300] and [0.01,0.9], respectively. Dark grey vertical bars display the first through third interquartile range, with the median represented by the white dot.

Table S5, Supporting information), with the latter exceeding the 100th percentile of the null distribution. To consider larger numbers of loci representative of the number of underlying loci estimated by BSLMM, we also isolated SNPs from the top 99.8th percentile of $\overline{PIP}$. In these sets, we found evidence for elevated signatures of selection acting across multiple loci for all phenotypes except for height, which did not produce a focal median $\hat{D}_{a(ij)}$ greater than the 95th percentile of null distribution of $\hat{D}_{a(ij)}$ (Fig. 4B, Table S5, Supporting information). When focal and null sets of SNPs were compared, focal sets were representative of single-locus (Fig. S16, Supporting information) and multilocus (Fig. S17, Supporting information) F_{ST} estimates of the null sets.

To identify signatures of allele frequency shifts among focal loci associated with phenotype ($pw\hat{D}_{a(ij)}$), we ran Mantel tests of $pw\hat{D}_{a(ij)}$ matrices against geographic distance and environmental Euclidian distance matrices. When considering SNPs identified by the 99.9th percentile of $\overline{PIP}$, we see substantial evidence for allele frequency shifts of loci associated with bu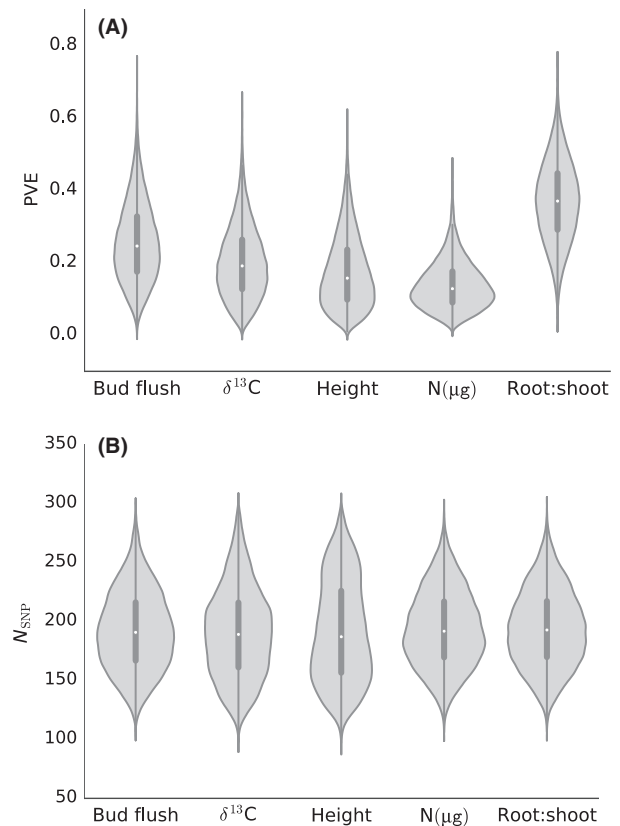d flush to Euclidian distances of GDD-May, GDD-Aug, per cent maximum radiation input, and minimum January temperature (Table 3). Additionally, when we consider the 99.8th percentile of $\overline{PIP}$, we show evidence for allele frequency shifts among loci associated with bud flush, height and δ^{13}C with Euclidian distances of annual precipitation, as well as for $N(\mu g)$ loci with elevation, and bud flush loci with both longitude (a correlate of annual precipitation) and per cent maximum radiation input (as in the 99.9th $\overline{PIP}$ set). The strong signal from bud flush and water-related variables in Table 3 is intriguing, as bud flush and δ^{13}C were the only two phenotypic traits to have significantly larger Q_{ST} than F_{ST} (P.E. Maloney, D.R. Vogler, A.J. Eckert, C.E. Jensen, A. Delfino-Mix, in review). The magnitude of the mean focal allele frequency differences across populations was subtle as expected (range: 0.054–0.087) and representative of unassociated SNPs of similar H_E (Fig. S18, Supporting information).
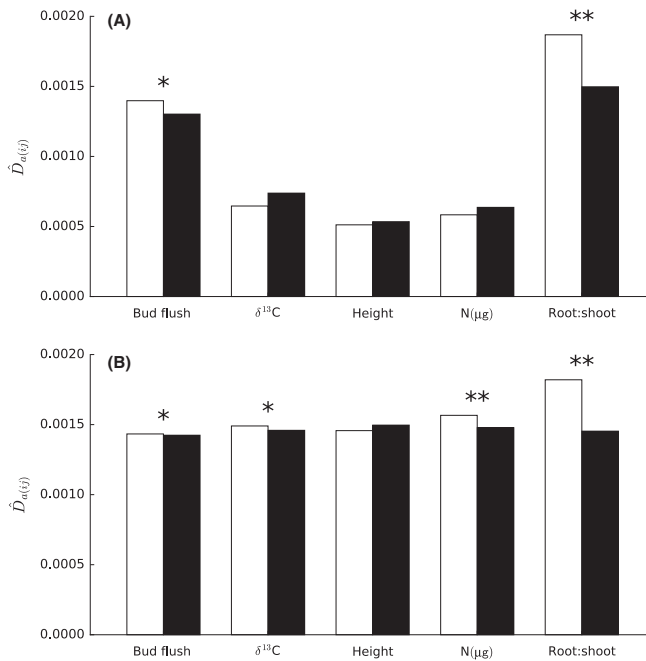
Fig. 4 Allele frequency covariance ($\hat{D}_{a(ij)}$) among loci associated to phenotype by GEMMA. In white are the median values from $\hat{D}_{a(ij)}$ calculated among focal SNPs associated with phenotype. Black bars display the 95th percentile of the null distribution of median. (A) SNPs identified in the top 99.9th percentile of $\overline{PIP}$, (B) SNPs identified in the top 99.8th percentile of $\hat{D}_{a(ij)}$. One star (*) indicates that the median focal $\hat{D}_{a(ij)}$ was greater than the 95th percentile of the null distribution, whereas two stars (**) indicate that the focal median $\hat{D}_{a(ij)}$ was greater than the 100th percentile of the null distribution.

F_{ST} outlier analysis

OUTFLANK analysis revealed 110 focal loci as outliers for F'_{ST} (range: 0.069–0.118). Expected heterozygosity values among the outlier SNPs (Fig. S19, Supporting information) varied across the distribution from the full set of SNPs (Fig. S5, Supporting information). Upon analysis of patterns of covariance ($\hat{D}_{a(ij)}$) among the OUTFLANK focal SNPs, we found that the median focal $\hat{D}_{a(ij)}$ (6.08e−03) was 10.6× greater than the 100th percentile of the null distribution of $\hat{D}_{a(ij)}$ (5.74e−04). However, when we analysed these outlier SNPs for signatures of allele frequency shifts ($pw\hat{D}_{a(ij)}$), we found no significant associations with geographic or environmental distances.

Assessing possible artefactual signals of high $\hat{D}_{a(ij)}$

It was of interest to determine whether the elevated $\hat{D}_{a(ij)}$ inferred for focal sets of loci identified from BAYENV2 and OUTFLANK was artefactual. For instance, loci identified by either method will likely covary in frequency as a result of the allele frequency differences among populations, perhaps elevating $\hat{D}_{a(ij)}$ within focal sets. To assess this possible artefact, we randomized individuals across populations 100 times while maintaining original sample sizes for each population, and reran OUTFLANK to classify outliers, as described previously. We found that outlier SNPs for all 100 randomizations displayed an elevated $\hat{D}_{a(ij)}$, as was the case with the original data. To determine whether the magnitude of the $\hat{D}_{a(ij)}$ estimate from our original OUTFLANK results was greater

than expected, we constructed a distribution by calculating this magnitude from each of the random runs by dividing the median focal $\hat{D}_{a(ij)}$ from the outlier set by the 100th percentile of the same run's null distribution. Using this distribution of 100 magnitudinal differences, we found that the elevated $\hat{D}_{a(ij)}$ calculated from our original set (10.6× greater than 100th percentile of the null) was 4.81 standard deviations from the mean of the distribution and 1.25× greater than the 100th percentile. This suggests that our original focal set from OUTFLANK still displayed significantly greater $\hat{D}_{a(ij)}$ even after methodological artefacts were taken into account. We did not perform a similar analysis with BAYENV2 because this was computationally prohibitive, but we expect similar patterns to have emerged. If we instead use the original results (Fig. 2) as a surrogate for null expectations, we find that the magnitudinal difference between focal and null $\hat{D}_{a(ij)}$ (as calculated above) for annual precipitation is 2.11 standard deviations from the mean of the distribution of differences from environmental associations. If we exclude the top three environmental variables with the largest differences (annual precipitation, GDD-Aug and Tmin-Jan; Fig. 2, Table S3, Supporting information), the difference for annual precipitation increases to 3.97 standard deviations from the mean. Because the signal for elevated $\hat{D}_{a(ij)}$ remains after accounting for artefacts, and given the other biological signals from our data set, we conclude that the results presented here are consistent with expected signals of local adaptation driven by water availability in this system.

Table 3 Signatures of allele frequency shifts associated with environmental distance. Significant Mantel tests (9999 permutations) from comparisons among allele frequency shifts ($pw\hat{D}_{a(ij)}$) of SNPs associated with phenotype (second column) against environmental Euclidian distance (third column). Selection criterion refers to the process used to identify SNPs associated with phenotype

Selection criterion	$pw\hat{D}_{a(ij)}$	Environmental Euclidian distance	Mantel's r	P-value
99.9th $\overline{PIP}$	Bud flush	GDD-August	0.5804	0.0181
	Bud flush	GDD-May	−0.5190	0.0458
	Bud flush	Max. radiation input	−0.5486	0.0482
	Bud flush	T_{min} January	0.6984	0.0191
99.8th $\overline{PIP}$	Bud flush*	Annual precipitation	0.4309	0.0140
	Bud flush*	Longitude	0.5532	0.0405
	Bud flush	Max. radiation input	−0.6312	0.0127
	N (µg)	Elevation	0.5334	0.0246
	Height*	Annual precipitation	0.7210	0.0320
	δ^{13}C*	Annual precipitation	0.5952	0.0195

*A comparison in which at least one variable is water-related, or was associated with annual precipitation.

Intersection of SNPs within and across methods

We examined overlap of focal SNPs among the various methods employed in this study (Table S7, Supporting information). While there was considerable overlap of loci found between methods, overall there was more overlap of loci associated with multiple phenotypes or with multiple environments than found across methods. For sets of loci associated with environmental variables, the overlap of loci among environments seemed to be driven by the correlations among soil properties, for when ordered by the number of loci within the intersection, 12 of the top 15 comparisons were among edaphic conditions (Table S7, Supporting information). Additionally, climate-related variables relating to maximum radiation input, degree growing days, minimum and maximum temperature generally shared loci among soil variables relating to water availability, while annual precipitation shared 18 loci with longitude, among other variables. Very few of the loci identified by BAYENV2 would have been detected through conventional F_{ST} outlier approaches (Figs S20–S21, Supporting information). Even so, OUTFLANK captured between 1 and 3 ($n = 18$) of the loci identified across 10 of the 18 environmental associations from BAYENV2, many of which were water-related (e.g., annual precipitation), and

captured 4 of the loci identified in the 99.8th percentile of $\overline{PIP}$, but not for any of the loci identified from the reduced threshold of LMM. Among loci associated with phenotype (99.8th $\overline{PIP}$), there were between one and three loci which were found in the intersection among pairwise phenotypic comparisons, yet none of these overlap loci were those identified from LMM. Finally, 15 loci associated with environment overlapped with the 99.8th percentile of $\overline{PIP}$ (including two between δ^{13}C and longitude, a correlate of annual precipitation), while environmental associations did not capture any of the reduced-threshold loci from univariate LMM (Table S7, Supporting information).

Discussion

The spatial extent of local adaptation, particularly in conifers, has generally been investigated at regional scales (Neale & Savolainen 2004; Savolainen *et al.* 2007; Ćalić *et al.* 2016). While informative for range-wide inference, management and conservation agencies are often limited to local scales spanning only tens to several hundreds of square kilometres. While there is an expectation that high gene flow (i.e. migration load) exhibited by many conifers can lead to swamping of adaptive alleles, there is mounting empirical evidence that adaptation to the environment can still occur at relatively fine spatial scales (Mitton *et al.* 1989, 1998; Budde *et al.* 2014; Csilléry *et al.* 2014; Vizcaíno-Palomar *et al.* 2014; Eckert *et al.* 2015; Holliday *et al.* 2016; Roschanksi *et al.* 2016). Thus, studies which investigate adaptation at scales amenable to management may be of relatively greater importance (especially for endangered and threatened species) to reforestation applications such as those carried out through seed sourcing (*sensu* McLane & Aitken 2012) and replanting efforts. Previously, we provided evidence that measured fitness-related phenotypes are heritable, that population explains a significant proportion of phenotypic variation, and Q_{ST} was significantly greater than F_{ST} for bud flush and δ^{13}C (P.E. Maloney, D.R. Vogler, A.J. Eckert, C.E. Jensen, A. Delfino-Mix, in review). Here, our genetic analyses indicate selective pressures of *Pinus albicaulis* are likely driven by water availability (e.g., precipitation gradients) as well as interactions and correlates of soil properties, which lends replicative support to both theoretical and empirical predictions for the patterns of loci underlying quantitative traits undergoing selection with gene flow. For instance, Ma *et al.* (2010) assessed evidence for diversifying selection within European aspen (*Populus tremula* L.) across 23 candidate genes of the photoperiodic pathway using the covariance of allelic effects among loci, albeit across a geographic region of Sweden spanning 10 latitudinal

degrees. From this candidate set, they identified high degrees of covariance among phenotypic effects as predicted from theory (Latta 1998), despite minimal allele frequency differentiation among sampled populations. More recently, Csilléry *et al.* (2014) assessed 53 climate-related candidate genes within European beech (*Fagus sylvatica* L.) providing evidence that covariance among loci is attributable to epistatic selection (*sensu* Ohta 1982) across fine spatial scales of less than 100 km^2. While varying across spatial scales, these studies replicate evidence for a signal of local adaptation in trees through elevated among-population linkage disequilibrium between adaptive loci.

Standing genetic variation for fitness-related traits

The populations under study appear to have extensive gene flow, recent divergence, or both. Variation of allele frequencies among populations accounts for less than 1% of the variance observed, which was less than that found for *P. lambertiana* populations within the LTB (Eckert *et al.* 2015), or among isozymes sampled from populations across the Northern *P. albicaulis* range (Krakowski *et al.* 2003). Inspection of PCs showed no distinctive clustering of populations (Fig. S2, Supporting information), while population pairwise F_{ST} did not exceed 0.016 and a test for isolation by distance was not significant. Consequently, the mean allele frequency differences between populations for focal SNPs were also subtle. Biologically, such a pattern of extensive sharing of alleles across populations has likely resulted from a combination of long-distance pollen movement, and seed dispersal by Clark's nutcracker (*Nucifraga columbiana* Wilson) which is known to disperse seeds at distances similar to those between our sampled populations (Tomback 1982; Richardson *et al.* 2002 and references therein). Given this pattern of structure, the island model with symmetric migration used to describe the interpopulation component of linkage disequilibrium among loci ($\hat{D}_{a(ij)}$) and allele frequency shifts ($pw\hat{D}_{a(ij)}$) is likely suitable to investigate our data set for signatures of selection across multiple loci.

While BAYENV2 did not identify any loci strongly associated with environment, as given from small values of Bayes factors (all $\overline{BF} < 1.0$, Table S3, Supporting information), there is a strong biological signal for adaptation to soil water availability in our data set (discussed below), evidence that other white pines within the LTB are also being structured by precipitation differences among populations (Eckert *et al.* 2015), and elevated signals of selection among focal loci associated to annual precipitation which would be unlikely to arise, given the data and methodological artefacts. Thus, it

seems unlikely that the focal sets of SNPs associated to annual precipitation, and perhaps GDD-Aug and Tmin-Jan, are driven solely by false positives. However, if the majority of loci associated with environment are not an artefact of the method (i.e., are within or in linkage with causative sites), one possible explanation for elevated covariance is that the structure of environmental variables across populations captured variation for unmeasured phenotypic traits which were largely representative of total lifetime fitness (Schoville *et al.* 2012). Structure of unmeasured fitness-related traits is also likely to explain the high covariance of OUTFLANK loci. Future work could provide validation through functional analyses of loci or from similar patterns found in other systems.

Water availability as a driver of local adaptation

The strongest signal for local adaptation among *P. albicaulis* populations of the LTB came from evidence of adaptation to soil water availability (Tables 2–3; Figs 2 and 4). Indeed, water availability is a critical component shaping standing variation across plant taxa (Vicente-Serrano *et al.* 2013), including the distributions of tree species in general (van Mantgem *et al.* 2009; Allen *et al.* 2010), and southern populations of *P. albicaulis* specifically (Bower & Aitken 2008; Chang *et al.* 2014). During the Pleistocene–Holocene transition (10 000–12 000 yr BP), shifts from mesic to xeric conditions caused proximal *P. albicaulis* populations of the Western Great Basin (~50 km distant) to shift from 1380 m in elevation to their current position about 1100 m downslope (Nowak *et al.* 1994; cf. Table 1). Such shifts in climate and local edaphic conditions in the last 10 000 years may in part explain recent (relative to $4N_e$ generations), and ongoing, selective pressures on *P. albicaulis* populations of the LTB. Because of climatic constraints imposed on the southern range of *P. albicaulis*, phenotypic traits affected by precipitation, soil water availability, or soil water capacity likely have fitness-related consequences for this species. Additionally, with climatic models predicting warmer temperatures, reduced snow accumulation, and earlier spring melt across the western USA, it is likely that *P. albicaulis* populations of the Sierra Nevada will continue to face selective pressures of this kind. Even so, many of *P. albicaulis* populations of the LTB exhibit substantial genetic variation for the fitness-related traits measured, suggesting that the majority of ongoing adaptation within the LTB will likely be unconstrained by the lack of genetic variation. Instead, other biotic factors (e.g., white pine-blister rust infection) that can lead to negative population growth rates may be of more immediate concern (see Maloney *et al.* 2012).

Implications to whitebark management

As pointed out by McLane & Aitken (2012), distribution models of many species predict habitat suitability to shift with climate in the upcoming century, leaving great uncertainty that tree species in particular will be able to track suitable environments through natural migration and establishment, as the rate of many of these geographic shifts would far exceed observed post-glacial rates of migration (Davis & Shaw 2001; McLachlan *et al.* 2005). Exacerbating this issue, the presence of *C. ribicola*, and climate-driven outbreaks of mountain pine beetle (*D. ponderosae*) create further challenges to the conservation of *P. albicaulis* (Tomback & Achuff 2010; Mahalovich & Stritch 2013). Without intervention, such cases could lead to population collapse, extirpation or extinction. As such, assisted gene flow, replanting or restoration efforts will need to continue to take current and future selective pressures into account (e.g., genetic variation, resistance to *C. ribicola*), as has generally been the standard of practice (Keane *et al.* 2012; Maloney *et al.* 2012; McLane & Aitken 2012).

At the same time, the choice of seed source will also need to take into account local adaptation at fine spatial scales. While a small proportion of the neutral genetic variation (F_{ST}) is found among most tree populations (often less than 5%, Neale & Savolainen 2004), this does not necessarily mean that seeds from within an established seed zone will be optimal for any given constituent environment, particularly if the seed zone exhibits high environmental heterogeneity (such as in montane regions), or if the seed zone is relatively broad compared to these environmental gradients, as is the case in California (see Buck *et al.* 1970). Weak neutral genetic differentiation can be misleading in this way, as polygenic traits influenced by selective processes in the face of gene flow may lead to divergent local adaptation through the covariance of alleles among populations without the build-up of substantial genetic differentiation at any given locus. Particularly, in cases where there is evidence of local adaptation, and when ethical (McLachlan *et al.* 2007), appropriate (considering, e.g., ecological or demographic factors), or plausible, seed source should come from local sources (i.e., relative to scales of geography and environmental gradients) to maximize adaptive potential (McKay & Latta 2002). This is particularly important when maximal fitness (e.g., reproductive output) is a priority for established trees, as while many genotypes may survive, realized phenotypes related to fitness may be suboptimal for a given environment. In cases where local seed sourcing is not plausible, perhaps due to isolation, or with prohibitively small population sizes, sources likely to perform well are also likely to come from highly correlated environments, particularly

if the populations are not highly diverged. In contrast, local seed source may be of lesser importance for populations existing over broad, relatively homogeneous environments. Optimal sources in these cases will also likely come from recently diverged populations (McKay & Latta 2002). With this taken into consideration, management may be able to prioritize populations for restoration through estimates of trait heritability, either through common garden experimentation or estimates from marker data, as estimates of genetic variation and structure alone may be misleading. For instance, heritability for $\delta^{13}C$ was near zero for the Rifle Peak population, as was the case for root:shoot ratio in Freel Peak and Little Roundtop, N (µg) in Rifle Peak, and height for four of six populations. While this could mean the presence of recent, strong natural selection, or, conversely, that these traits do not convey an overwhelming adaptive advantage in these populations, candidate traits with substantial evidence for contributing to total lifetime fitness should be monitored nonetheless. In appropriate cases, introducing compatible variation would stand to improve adaptive potential in such populations. While there is no one specific solution to conserve populations of *P. albicaulis* across its range, taking into consideration fine-scale local adaptation in addition to established strategies will likely aid in such endeavours.

Limitations and concluding remarks

While we described associations among genotype, phenotype, and environment that collectively represent strong evidence for adaptive responses of *P. albicaulis* populations to the environment, we acknowledge several limitations. First, our study design was limited in statistical power which could have been improved by increasing the number of individuals sampled, the total number of populations, or both, given an ideal sampling regime (Lotterhos & Whitlock 2015). This would have facilitated use of other methodologies for uncovering evidence of polygenic local adaptation (e.g., Berg & Coop 2014). Second, while we measured fitness-related traits among seedlings of a species whose lifespan differs by several orders of magnitude, establishment success is one of the primary factors influencing dynamics of forest populations, and early life stages of plants have been shown to be a major component of total lifetime fitness (Postma & Ågren 2016). Third, much of the statistical signal for the association of allele frequency shifts to environment would be lost with correction for multiple tests. However, we leverage the fact that, of the few significant $pw\hat{D}_{a(ij)}$ associations, the majority were related to $\delta^{13}C$, annual precipitation, its correlate of longitude, or measures of soil water availability, which is an outcome highly unlikely by chance alone.

Fourth, while we provide evidence for statistical signals predicted by theory, our methodology limited us from making conclusions regarding local adaptation *sensu stricto* as we utilized just a single common garden without reciprocal transplants and were unable to quantify functional differences of putative loci among populations. Finally, a more fully curated, well-annotated genome assembly and accompanying linkage map would have aided in the detection of physical linkage among SNPs, proximity to genomic regions of estimated effect and detection of false positives. For instance, the *P. lambertiana* genome used to judge authenticity of sequence data does not yet have the density of annotation needed to draw inferences on the causative sites likely within or linked to the loci described here, as its assembly and curation are still ongoing. We cannot, therefore, conclude that elevated covariances inferred for focal loci are not an artefact due to distant linkage with causative sites of larger effect. For this artefact to be true, however, our results would indicate that many of the loci in focal sets of SNPs would all have to be linked to the same smaller number of larger-effect loci or that many large-effect loci underlie the measured traits, both unlikely outcomes given the expectations of quantitative traits and the coverage from ddRADseq methods found in other white pines (e.g., Friedline *et al.* 2015). Lastly, while we may not have solely identified causative sites, but instead those linked to causative genomic regions, linked sites can still maintain signals of evolutionary processes (McVean 2007). Future work could address these limitations and lead to the corroboration of our results, particularly in describing patterns exhibited by underlying loci in similar systems.

Our inferences were synthesized from prevailing signals across multiple phenotypic, environmental, and taxonomic (cf. Eckert *et al.* 2015) lines of evidence. The results reported here suggest that focal loci collectively show elevated allele frequency covariance (a signal expected between loci undergoing selection with gene flow) across multiple loci than could have been expected to arise from the data by chance or artefact and that interpopulation levels of allele frequency covariance are often associated with interpopulation distances of soil water availability. Our results further explain a considerable proportion (*PVE*) of the additive genetic variation (h^2) of the quantitative traits under study from a polygenic perspective, as should be the case with sufficient genetic sampling (Gompert *et al.* 2016). Thus, we can posit that the general mode of adaptation for *P. albicaulis* across the LTB is facilitated by selection on standing levels of genetic variation that is extensively shared throughout the basin and likely improves performance in early life stages. Finally, if soil and climatic variables continue to influence the extant populations within the LTB as evidenced from our analyses, it is likely that these variables will continue to be important to the long-term success of this threatened keystone species.

References

Allen CD, Macalady AK, Chenchouni H *et al.* (2010) A global overview of drought and heat-induced tree mortality reveals emerging climate change risks for forests. *Forest Ecology and Management*, **259**, 660–684.

Barrett R, Schluter D (2008) Adaptation from standing genetic variation. *Trends in Ecology & Evolution*, **23**, 38–44.

Barton NH (1999) Clines in polygenic traits. *Genetical Research*, **74**, 223–236.

Berg JJ, Coop G (2014) A population genetic signal of polygenic adaptation. *PLoS Genetics*, **10**, e1004412.

Bourret V, Dionne M, Bernatchez L (2014) Detecting genotypic changes associated with selective mortality at sea in Atlantic salmon: polygenic multilocus analysis surpasses genome scan. *Molecular Ecology*, **23**, 4444–4457.

Bower AD, Aitken SN (2008) Ecological genetics and seed transfer guidelines for *Pinus albicaulis* (Pinaceae). *American Journal of Botany*, **95**, 66–76.

Buck JM, Adams RS, Cone J *et al.* (1970) *California Seed Zones*, p. 5. California Region, Forest Service, United States Department of Agriculture, San Francisco.

Budde KB, Heuertz M, Hernández-Serrano A *et al.* (2014) In situ genetic association for serotiny, a fire-related trait, in Mediterranean maritime pine (*Pinus pinaster*). *New Phytologist*, **201**, 230–241.

Ćalić I, Bussotti F, Martínez-García PJ, Neale DB (2016) Recent landscape genomics studies in forest trees. *Tree Genetics & Genomes*, **12**, 1–7.

Chang T, Hansen AJ, Piekielek N (2014) Patterns and variability of projected bioclimatic habitat for *Pinus albicaulis* in the greater Yellowstone Area (B Bond-Lamberty, Ed.). *PLoS ONE*, **9**, e111669.

Comeault AA, Soria-Carrasco V, Gompert Z *et al.* (2014) Genome-wide association mapping of phenotypic traits subject to a range of intensities of natural selection in *Timema cristinae*. *The American Naturalist*, **183**, 711–727.

Comeault AA, Flaxman SM, Riesch R *et al.* (2015) Selection on a genetic polymorphism counteracts ecological speciation in a stick insect. *Current Biology*, **25**, 1975–1981.

Coop G, Witonsky D, Di Rienzo A, Pritchard JK (2010) Using environmental correlations to identify loci underlying local adaptation. *Genetics*, **185**, 1411–1423.

Csilléry K, Lalagüe H, Vendramin GG, González-Martínez SC, Fady B, Oddou-Muratorio S (2014) Detecting short spatial scale local adaptation and epistatic selection in climate-related candidate genes in European beech (*Fagus sylvatica*) populations. *Molecular Ecology*, **23**, 4696–4708.

Daly C, Neilson RP, Phillips DL (1994) A statistical-topographic model for mapping climatological precipitation over mountainous terrain. *Journal of Applied Meteorology*, **33**, 140–158.

Davis MB, Shaw RG (2001) Range shifts and adaptive responses to quaternary climate change. *Science*, **292**, 673–679.

Eckert AJ, Wegrzyn JL, Pande B *et al.* (2009) Multilocus patterns of nucleotide diversity and divergence reveal positive selection at candidate genes related to cold hardiness in coastal Douglas fir (*Pseudotsuga menziesii var. menziesii*). *Genetics*, **183**, 289–298.

Eckert AJ, van Heerwaarden J, Wegrzyn JL *et al.* (2010) Patterns of population structure and environmental associations to aridity across the range of loblolly pine (*Pinus taeda* L., Pinaceae). *Genetics*, **185**, 969–982.

Eckert AJ, Maloney PE, Vogler DR, Jensen CE, Mix AD, Neale DB (2015) Local adaptation at fine spatial scales: an example from sugar pine (*Pinus lambertiana*, Pinaceae). *Tree Genetics & Genomes*, **11**, 1–17.

Ehret GB, Lamparter D, Hoggart CJ, Whittaker JC, Beckmann JS, Kutalik Z, Genetic Investigation of Anthropometric Traits Consortium (2012) A multi-SNP locus-association method reveals a substantial fraction of the missing heritability. *The American Journal of Human Genetics*, **91**, 863–871.

Endler JA (1977) *Geographic Variation, Speciation, and Clines*. No. 10. Princeton University Press, Princeton.

Friedline CJ, Lind BM, Hobson EM *et al.* (2015) The genetic architecture of local adaptation I: the genomic landscape of foxtail pine (*Pinus balfouriana* Grev. & Balf.) as revealed from a high-density linkage map. *Tree Genetics & Genomes*, **11**, 1–15.

Gompert Z, Jahner JP, Scholl CF *et al.* (2015) The evolution of novel host use is unlikely to be constrained by trade-offs or a lack of genetic variation. *Molecular Ecology*, **24**, 2777–2793.

Gompert Z, Egan SP, Barret RDH, Feder JL, Nosil P (2016) Multilocus approaches for the measurement of selection on correlated genetic loci. *Molecular Ecology*, **26**, 1–18.

González-Martínez SC, Huber D, Ersoz E, Davis JM, Neale DB (2008) Association genetics in *Pinus taeda* L. II. Carbon isotope discrimination. *Heredity*, **101**, 19–26.

Guan Y, Stephens M (2011) Bayesian variable selection regression for genome-wide association studies and other large-scale problems. *Annals of Applied Statistics*, **5**, 1780–1815.

Günther T, Coop G (2013) Robust identification of local adaptation from allele frequencies. *Genetics*, **195**, 205–220.

Haasl RJ, Payseur BA (2016) Fifteen years of genomewide scans for selection: trends, lessons and unaddressed genetic sources of complication. *Molecular Ecology*, **25**, 5–23.

Hall D, Luquez V, Garcia VM, St Onge KR, Jansson S, Ingvarsson PK (2007) Adaptive population differentiation in phenology across a latitudinal gradient in European aspen (*Populus tremula*, L.): a comparison of neutral markers, candidate genes, and phenotypic traits. *Evolution*, **61**, 2849–2860.

Hermisson J, Pennings PS (2005) Soft sweeps: molecular population genetics of adaptation from standing genetic variation. *Genetics*, **169**, 2335–2352.

Holland J (2007) Genetic architecture of complex traits in plants. *Current Opinion in Plant Biology*, **10**, 156–161.

Holliday JA, Zhou L, Bawa R, Zhang M, Oubida RW (2016) Evidence for extensive parallelism but divergent genomic architecture of adaptation along altitudinal and latitudinal gradients in *Populus trichocarpa*. *New Phytologist*, **209**, 1240–1251.

Hornoy B, Pavy N, Gérardi S, Beaulieu J, Bousquet J (2015) Genetic adaptation to climate in white spruce involves small to moderate allele frequency shifts in functionally diverse genes. *Genome Biology and Evolution*, **7**, 3269–3285.

Keane RE, Tomback DF, Aubry CA *et al.* (2012) A range-wide restoration strategy for whitebark pine (*Pinus albicaulis*). United States Department of Agriculture Forest Service Rocky Mountain Research Station General Technical Report RMRS-GTR-279.

Kemper KE, Saxton SJ, Bolormaa S, Hayes BJ, Goddard ME (2014) Selection for complex traits leaves little or no classic signatures of selection. *BMC Genomics*, **15**, 246–260.

Krakowski J, Aitken SN, El-Kassaby YA (2003) Inbreeding and conservation genetics in whitebark pine. *Conservation Genetics*, **4**, 581–593.

Kremer A, Le Corre V (2012) Decoupling of differentiation between traits and their underlying genes in response to divergent selection. *Heredity*, **108**, 375–385.

Langlet O (1971) Two hundred years of genecology. *Taxon*, **20**, 653–721.

Latta RG (1998) Differentiation of allelic frequencies at quantitative trait loci affecting locally adaptive traits. *The American Naturalist*, **151**, 283–292.

Latta RG (2003) Gene flow, adaptive population divergence and comparative population structure across loci. *New Phytologist*, **161**, 51–58.

Le Corre V, Kremer A (2003) Genetic variability at neutral markers, quantitative trait loci and trait in a subdivided population under selection. *Genetics*, **164**, 1205–1219.

Le Corre V, Kremer A (2012) The genetic differentiation at quantitative trait loci under local adaptation. *Molecular Ecology*, **21**, 1548–1566.

Lotterhos KE, Whitlock MC (2015) The relative power of genome scans to detect local adaptation depends on sampling design and statistical method. *Molecular Ecology*, **24**, 1031–1046.

Luquez V, Hall D, Albrectsen BR, Karlsson J, Ingvarsson P, Jansson S (2007) Natural phenological variation in aspen (*Populus tremula*): the SwAsp collection. *Tree Genetics & Genomes*, **4**, 279–292.

Ma XF, Hall D, Onge KRS, Jansson S, Ingvarsson PK (2010) Genetic differentiation, clinal variation and phenotypic associations with growth cessation across the *Populus tremula* photoperiodic pathway. *Genetics*, **186**, 1033–1044.

Mackay TFC, Stone EA, Ayroles JF (2009) The genetics of quantitative traits: challenges and prospects. *Nature Reviews Genetics*, **10**, 565–577.

Mahalovich MF, Stritch L (2013) *Pinus albicaulis*. The IUCN Red List of Threatened Species. e.T39049A2885918. https://doi.org/10.2305/IUCN.UK.2013-1.RLTS.T39049A2885918.en.

Maloney PE, Vogler DR, Eckert AJ, Jensen CE, Delfino-Mix A (2012) Ecology of whitebark pine in relation to white pine-blister rust infection in subalpine forests of the Lake Tahoe Basin, USA: implications for restoration. *Forest Ecology and Management*, **280**, 166–175.

Mantel N (1967) The detection of disease clustering and a generalized regression approach. *Cancer Research*, **27**, 209–220.

van Mantgem PJ, Stephenson NL, Byrne JC *et al.* (2009) Widespread increase of tree mortality in the western United States. *Science*, **323**, 521–524.

McKay JK, Latta RG (2002) Adaptive population divergence: markers, QTL and traits. *Trends in Ecology & Evolution*, **17**, 285–291.

McLachlan JS, Clark JS, Manos PS (2005) Molecular indicators of tree migration capacity under rapid climate change. *Ecology*, **86**, 2088–2098.

McLachlan JS, Hellman JJ, Schwartz MW (2007) A framework for debate of assisted migration in an era of climate change. *Conservation Biology*, **21**, 297–302.

McLane SC, Aitken SN (2012) Whitebark pine (*Pinus albicaulis*) assisted migration potential: testing establishment north of the species range. *Ecological Applications*, **22**, 142–153.

McVean G (2007) The structure of linkage disequilibrium around a selective sweep. *Genetics*, **175**, 1395–1406.

Mitton JB, Stutz HP, Schuster WS (1989) Genotypic differentiation at PGM in Engelmann spruce from wet and dry sites. *Silvae Genetica*, **38**, 217–221.

Mitton JB, Grant MC, Yoshino AM (1998) Variation in allozymes and stomatal size in pinyon (*Pinus edulis*, Pinaceae), associated with soil moisture. *American Journal of Botany*, **85**, 1262–1265.

Moser G, Lee SH, Hayes BJ, Goddard ME, Wray NR, Visscher PM (2015) Simultaneous discovery, estimation and prediction analysis of complex traits using a Bayesian mixture model. *PLoS Genetics*, **11**, e1004969.

Neale DB, Savolainen O (2004) Association genetics of complex traits in conifers. *Trends in Plant Science*, **9**, 325–330.

Nowak CL, Nowak RS, Tausch RJ, Wigand PE (1994) A 30000 year record of vegetation dynamics at a semi-arid locale in the Great Basin. *Journal of Vegetation Science*, **5**, 579–590.

Ohta T (1982) Linkage disequilibrium with the island model. *Genetics*, **101**, 139–155.

Parchman TL, Gompert Z, Mudge J, Schilkey FD, Benkman CW, Buerkle CA (2012) Genome-wide association genetics of an adaptive trait in lodgepole pine. *Molecular Ecology*, **21**, 2991–3005.

Patterson N, Price AL, Reich D (2006) Population structure and eigenanalysis. *PLoS Genetics*, **2**, e190.

Pérez F, Granger BE (2007) IPython: a system for interactive scientific computing. *Computing in Science and Engineering*, **9**, 21–29.

Peterson BK, Weber JN, Kay EH, Fisher HS, Hoekstra HE (2012) Double digest RADseq: an inexpensive method for de novo SNP discovery and genotyping in model and non-model species. *PLoS ONE*, **7**, e37135.

Postma FM, Ågren J (2016) Early life stages contribute strongly to local adaptation in Arabidopsis thaliana. *Proceedings of the National Academy of Sciences*, **113**, 7590–7595.

Pritchard JK, Di Rienzo A (2010) Adaptation – not by sweeps alone. *Nature Reviews Genetics*, **11**, 665–667.

R Core Team (2015) *R: A Language and Environment for Statistical Computing.* R Foundation for Statistical Computing, Vienna, Austria. http://wwwR-projectorg/

Richardson BA, Brunsfeld SJ, Klopfenstein NB (2002) DNA from bird-dispersed seed and wind-disseminated pollen provides insights into postglacial colonization and population genetic structure of whitebark pine (*Pinus albicaulis*). *Molecular Ecology*, **11**, 215–227.

Richardson JL, Urban MC, Bolnick DI, Skelly DK (2014) Microgeographic adaptation and the spatial scale of evolution. *Trends in Ecology & Evolution*, **29**, 165–176.

Roschanksi AM, Csillery K, Liepelt S *et al.* (2016) Evidence of divergent selection at landscape and local scales in *Abies alba* Mill. in the French Mediterranean Alps. *Molecular Ecology*, **25**, 776–794.

Savolainen O, Pyhäjärvi T (2007) Genomic diversity in forest trees. *Current Opinion in Plant Biology*, **10**, 162–167.

Savolainen O, Pyhäjärvi T, Knürr T (2007) Gene flow and local adaptation in trees. *Annual Review of Ecology, Evolution, and Systematics*, **38**, 595–619.

Savolainen O, Lascoux M, Merilä J (2013) Ecological genomics of local adaptation. *Nature Reviews Genetics*, **14**, 807–820.

Schoville SD, Bonin A, Francois O, Lobreaux S, Melodelima C, Manel S (2012) Adaptive genetic variation on the landscape: methods and cases. *Annual Review of Ecology, Evolution, and Systematics*, **43**, 23–43.

Sork VL, Aitken SN, Dyer RJ, Eckert AJ, Legendre P, Neale DB (2013) Putting the landscape into the genomics of trees: approaches for understanding local adaptation and population responses to changing climate. *Tree Genetics & Genomes*, **9**, 901–911.

Stephan W (2015) Signatures of positive selection: from selective sweeps at individual loci to subtle allele frequency changes in polygenic adaptation. *Molecular Ecology*, **25**, 79–88.

Storey JD, Bass AJ, Dabney A, Robinson D (2015) qvalue: Q-value estimation for false discovery rate control R package version 2.4.2.

Storz JF (2005) Using genome scans of DNA polymorphism to infer adaptive population divergence. *Molecular Ecology*, **14**, 671–688.

Storz JF, Kelly JK (2008) Effects of spatially varying selection on nucleotide diversity and linkage disequilibrium: insights from deer mouse globin genes. *Genetics*, **180**, 367–379.

Tiffin P, Ross-Ibarra J (2014) Advances and limits of using population genetics to understand local adaptation. *Trends in Ecology & Evolution*, **29**, 673–680.

Tigano A, Friesen VL (2016) Genomics of local adaptation with gene flow. *Molecular Ecology AOP*, **25**, 1–21.

Tomback DF (1982) Dispersal of whitebark pine seeds by Clark's nutcracker: a mutualism hypothesis. *The Journal of Animal Ecology*, **51**, 451–467.

Tomback DF, Achuff P (2010) Blister rust and western forest biodiversity: ecology, values and outlook for white pines. *Forest Pathology*, **40**, 186–225.

Tomback DF, Resler LM, Keane RE, Pansing ER, Andrade AJ, Wagner AC (2016) Community structure, biodiversity, and ecosystem services in treeline whitebark pine communities: potential impacts from a non-native pathogen. *Forests*, **7**, 1–8.

Turchin MC, Chiang CW, Palmer CD, Sankararaman S, Reich D, Hirschhorn JN (2012) Evidence of widespread selection

on standing variation in Europe at height-associated SNPs. *Nature Genetics*, **44**, 1015–1019.

USDA Forest Service, *Forest Health Technology Enterprise Team* Ft Collins, CO. Available at: https://www.fs.fed.us/foresthealth/technology/

United States Department of Agriculture, Natural Resources Conservation Service (2007) *Soil Survey of the Tahoe Basin Area, California and Nevada* Available at: http://soils.usda.gov/survey/printed_surveys/.

Vicente-Serrano SM, Gouveia C, Camarero JJ *et al.* (2013) Response of vegetation to drought time-scales across global land biomes. *Proceedings of the National Academy of Sciences*, **110**, 52–57.

Vizcaíno-Palomar N, Revuelta-Eugercios B, Zavala MA, Alia R, González-Martínez SC (2014) The role of population origin and microenvironment in seedling emergence and early survival in Mediterranean maritime pine (*Pinus pinaster* Aiton). *PLoS ONE*, **9**, e109132.

Weir BC, Cockerham CC (1984) Estimating F-statistics for the analysis of population structure. *Evolution*, **38**, 1358–1370.

Whitlock MC, Lotterhos KE (2015) Reliable detection of loci responsible for local adaptation: inference of a null model through trimming the distribution of FST. *The American Naturalist*, **186**, S24–S36.

Yeaman S, Whitlock MC (2011) The genetic architecture of adaptation under migration-selection balance. *Evolution*, **65**, 1897–1911.

Zhou X, Carbonetto P, Stephens M (2013) Polygenic modeling with Bayesian sparse linear mixed models. *PLoS Genetics*, **9**, e1003264.

Data accessibility

Sequence data are deposited in the Short Read Archive of the National Center for Bio-technology Information (project number: PRJNA377566). Scripts used in analyses can be found in IPython notebook format (Pérez & Granger 2007) at https://github.com/brandonlind/whitebark_pine. Included as a supplemental file are the final genotype calls based on minor allele counts. This file also includes raw phenotype, population, and plot data.

Supporting information

Additional supporting information may be found in the online version of this article.

Fig. S1 Single-locus F_{ST} for all SNPs (N = 116 231) calculated from HIERFSTAT. 95% CI: -0.0289, 0.0428.

Fig. S2 Principal component analysis of allele frequencies for the empirical dataset imputed with Beagle.

Fig. S3 Distributions of expected heterozygosity across BAYENV2 focal loci for 9/18 environments.

Fig. S4 Distributions of expected heterozygosity across BAYENV2 focal loci for 9/18 environments.

Fig. S5 Expected heterozygosity across all loci in the empirical set of SNPs (n = 116 231).

Fig. S6 Comparison of single-locus F_{ST} between focal sets of SNPs from BAYENV2 analysis and corresponding null groups.

Fig. S7 Comparison of single-locus F_{ST} between focal sets of SNPs from BAYENV2 analysis and corresponding null groups.

Fig. S8 Comparison of multilocus F_{ST} between focal sets of SNPs from BAYENV2 analysis and corresponding null groups.

Fig. S9 Comparison of multilocus F_{ST} between focal sets of SNPs from BAYENV2 analysis and corresponding null groups.

Fig. S10 Mean allele frequency difference ($\overline{\Delta p}$) among 8 populations for focal loci associated to environment (red line) by BAYENV2 and from 1000 sets of random SNPs chosen by H_E (black distributions).

Fig. S11 Mean allele frequency difference ($\overline{\Delta p}$) among 8 populations for focal loci associated to environment (red line) by BAYENV2 and from 1000 sets of random SNPs chosen by H_E (black distributions).

Fig. S12 Distributions of the harmonic mean posterior inclusion probability $\overline{PIP}$ ($\bar{\gamma}$) for loci identified by the 99.9th or the 99.8th percentile of $\overline{PIP}$ estimated from BSLMM.

Fig. S13 Expected heterozygosity across focal (≥99.9th percentile of $\overline{PIP}$) loci identified by BSLMM.

Fig. S14 Expected heterozygosity across focal (≥99.8th percentile of $\overline{PIP}$) loci identified by BSLMM.

Fig. S15 *P*-values from Wald's tests used in single-locus phenotypic association implemented through univariate LMM using the GEMMA software package.

Fig. S16 Comparison of single-locus F_{ST} between focal sets of SNPs from GEMMA analysis and corresponding null groups.

Fig. S17 Comparison of multilocus F_{ST} between focal sets of SNPs from GEMMA analysis and corresponding null groups.

Fig. S18 Mean allele frequency difference ($\overline{\Delta p}$) among 6 populations for focal loci associated to phenotype (red line) by BSLMM (≥99.8th percentile of $\overline{PIP}$) and from 1000 sets of random SNPs chosen by H_E (black distributions).

Fig. S19 Expected heterozygosity across focal SNPs from OutFLANK (n = 110).

Fig. S20 Histograms of single locus F_{ST} (blue bars) as calculated with HIERFSTAT for all SNPs (N = 116 231).

Fig. S21 Histograms of single locus F_{ST} (blue bars) as calculated with HIERFSTAT for all SNPs (N = 116 231).

Fig. S22 Effect size distributions of main effect ($\bar{\beta}$) for loci identified by the 99.9th or the 99.8th percentile of $\overline{PIP}$ estimated from BSLMM.

Fig. S23 Effect size distributions of sparse effect ($\bar{\alpha}$) for loci identified by the 99.9th or the 99.8th percentile of $\overline{PIP}$ estimated from BSLMM.

Fig. S24 Effect size distributions of total effect ($\hat{b} = \bar{\alpha} + \bar{\beta} \cdot \overline{PIP}$) for loci of the 99.9th or the 99.8th percentile of $\overline{PIP}$ estimated from BSLMM.

Fig. S25 Violin plots for main effects ($\bar{\alpha}$), sparse effects ($\bar{\beta}$), the posterior inclusion probability ($\overline{PIP}$), and model averaged effects ($\hat{b} = \bar{\alpha}_i + \bar{\beta}_i\overline{PIP}_i$) estimated in BSLMM.

Table S1 Degree of missing data across SNPs in dataset. Count (n) and fraction of all loci (N = 161 231) by bin.

Table S2 Environmental and phenotypic correlations.

Table S3 Results from genotype-environment association with BAYENV2.

Table S4 Parameter estimates of the mean (95% credible intervals) from GEMMA, except for h^2 and Q_{ST} (mean and 95% confidence interval - estimated in Maloney *et al.* in review).

Table S5 Results from genotype-phenotype associations. Covariation ($\hat{D}_{a(ij)}$) among *N* adaptive loci identified from the top percentiles of the harmonic mean posterior inclusion probability ($\overline{PIP}$) estimated from GEMMA.

Table S6 Results of univariate linear mixed models (LMM) as implemented in GEMMA.

Table S7 Intersection of SNPs among methods and the number of large-effect SNPs within the intersection.